J Mater Sci (2008) 43:4330–4339
DOI 10.1007/s10853-008-2637-7

Rolling wear of EPDM and SBR rubbers as a function of carbon black contents: correlation with microhardness

D. Xu · J. Karger-Kocsis · A. K. Schlarb

Received: 23 November 2007 / Accepted: 7 April 2008 / Published online: 17 April 2008

Abstract The rolling friction and wear of ethylene/propylene/diene (EPDM) and styrene/butadiene rubbers (SBR) with different carbon black (CB) contents were studied against steel in orbital rolling ball (steel)-on-plate (rubber) test rig (Orbital-RBOP) and oscillating rolling ball (steel)-on-plate (rubber) set-up (Oscillating-RBOP). The universal hardness (H), coefficient of friction (COF), and specific wear rate (W_s) of EPDM and SBR were determined. Incorporation of CB increases the universal hardness and the COF (the latter marginally) and decreases the specific wear rate for both EPDM and SBR. The wear mechanisms were concluded by inspecting the worn surfaces in scanning electron microscope and discussed as a function of CB modification. An inverse relationship between the specific wear rate and universal hardness was proposed in form of $W_s = kH^{-n}$, where k and n are constants for a given rubber and testing condition.

Introduction

Ethylene/propylene/diene (EPDM) and styrene/butadiene (SBR) rubbers have a wide range of applications, such as seals, conveying, belts, electrical insulators, tires, tubes, gaskets, etc. These applications drive research and developing activities to solve practical problems and to improve the performance of the above rubbers in the related parts. Considering the sliding friction and wear, a large body of research work was dedicated to related topics. Slusarski et al. [1] and Wildberger et al. [2] used various surface modifications to improve the friction properties of EPDM and SBR. Hong et al. [3] investigated the effects of the particle size and structure of various carbon blacks (CBs) on the friction and abrasion behavior of SBR. The friction behavior of the modified EPDM over a range of normal loads, temperatures, and sliding speeds has been studied and explained in terms of different mechanisms of rubber friction by Majumder and Bhowmick [4]. Interested readers can find useful information about the mechanical properties, sliding friction, wear characteristics, and sliding friction laws of polymers and rubbers in the books of Zhang [5], Friedrich [6], and Bayer [7]. Thavamani et al. [8, 9] studied the mechanisms of wear of SBR abraded against different counterparts under different conditions.

As to rolling-sliding friction, Iwai et al. [10] addressed this issue about SBR in a recent paper. However, still little information is available on the friction and wear under rolling and rolling-sliding conditions, especially when compared to results achieved in sliding and abrasion tests. So, in order to get funded knowledge on the rolling friction, wear and the related wear mechanisms need to be investigated in depth.

In this article, the dry rolling friction and wear of CB containing EPDM and SBR were studied against steel using orbital rolling ball (steel)-on-plate (RBOP) (Orbital-RBOP) and oscillating rolling ball-on-plate (Oscillating-RBOP) test rigs. The "plate" was the rubber in both above test configurations. The coefficient of friction (COF) and specific wear rate of EPDM and SBR were determined. The wear mechanisms were concluded by inspecting the worn surfaces by scanning electron microscopy (SEM) and discussed. An inverse relationship between the specific wear rate and universal hardness was proposed based on the results gained.

D. Xu · J. Karger-Kocsis (✉) · A. K. Schlarb
Institut für Verbundwerkstoffe GmbH (Institute for Composite Materials), Kaiserslautern University of Technology, Erwin Schrödinger Str. 58, 67663 Kaiserslautern, Germany
e-mail: karger@ivw.uni-kl.de

Experimental

EPDM and SBR rubbers

The rubber stocks were prepared in a laboratory internal mixer and the curatives were introduced on a laboratory open mill. The EPDM recipe used was as follows: EPDM (Keltan® 512 of DSM Elastomers, Sittard, The Netherlands): 100 part; carbon black (N550): 0, 30, 45, and 60 part; ZnO: 5 part; stearic acid: 1 part; sulfur: 1.5 part; *N*-cyclohexyl-2-benzothiazole sulfenamide (CBS, Vulkacit CZ of Bayer, Leverkusen, Germany): 0.6 part; 2-mercapto benzothiazole (MBT, Vulkacit Mercapto by Bayer): 0.6 part; zinc dicyanatodiamine (Rhenogran Geniplex 80 of Rhein Chemie, Mannheim, Germany): 0.6 part; zinc dibenzyl dithiocarbamate (Rhenogran ZBEC-70 of Rhein Chemie): 1.5 part. The SBR was produced without antioxidant and contained: SBR rubber (Krylene® 1500 of Lanxess, Pittsburgh, PA, USA): 100 part; CB (N330): 0, 30, 45, and 60 part; ZnO: 3 part; stearic acid: 1 part; sulfur: 1.5 part and CBS: 1.5 part. Note that the CB content was varied between 0 and 60 parts per hundred part rubber (phr) in both rubbers. Rubber sheets (ca. 2 mm thick) were produced by compression molding at 160 °C and 7 MPa pressure using a laboratory press (Weber, Remshalden, Germany). The vulcanization time was selected by considering the thickness of the specimens and the time needed for the 90% crosslinking of the rubber at $T = 160$ °C. The latter time was deduced from the torque–time curves registered by Monsanto moving die rheometer (MDR 2000 EA-1). The rubbers are further on referred with their CB content (the last digits in the designations represent the CB contents).

Hardness test [11]

Hardness is defined as the resistance of a solid material against the penetration of another harder material. In this article, the universal hardness testing has been followed according to the DIN 50359 standard. The universal hardness (H) is defined as the testing force divided by the apparent area of the indentation produced. Note that this hardness value was chosen as it informs us about the surface hardness (<15 μm thickness as a function of the CB content) which is subjected to the sliding-rolling wear.

Wear test

Friction and wear characteristics were determined in RBOP configurations in home-built devices. The rubber sheet was worn by one steel ball (100Cr6, diameter: 14 mm, arithmetical roughness R_a: 1 μm). In Orbital-RBOP configuration, the ball rolls along a circular path (diameter: 33 mm) when pushed against the rubber sheet with a given load. The following testing parameters were adopted in this configuration—normal load: 150 N, revolution: 300 rpm (corresponds to a speed of 0.52 m/s), duration: 3 h.

In Oscillating-RBOP configuration, the reciprocating linear rolling of the ball occurs at a frequency of 1 Hz with peak-to-peak amplitude of 25.06 mm (corresponds to a speed of 0.03 m/s) under the load 150 N for 6 h.

These two devices could record the COF as a function of time. The specific wear rate was calculated by:

$$W_s = \frac{\Delta V}{F \cdot L} \tag{1}$$

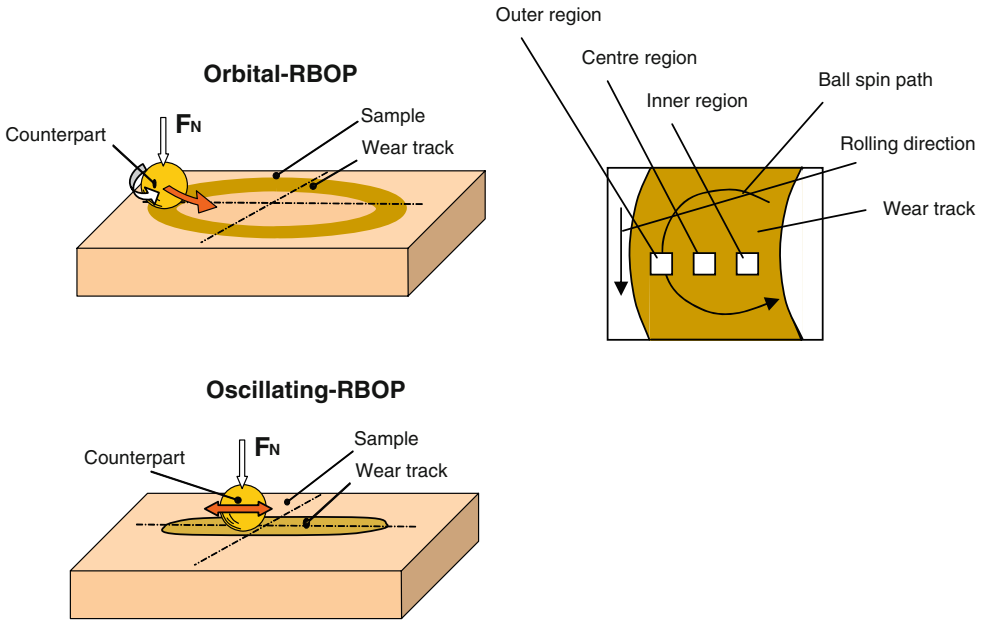

Fig. 1 Schemes of the test configurations of Orbital-RBOP (upper) and Oscillating-RBOP (lower). This figure also shows the preparation of the samples for SEM investigations after Orbital-RBOP test

where ΔV [mm^3] is the volume loss, F [N] is the normal load, and L [m] is the overall rolling distance. The loss volume (ΔV) was computed by measuring the width and depth of the wear track, assessed by a white light profilometer (see later) with the approximation that the cross section of the wear track was a half ellipse.

The test set-ups of the above testing methods are depicted schematically in Fig. 1.

Wear mechanisms

The worn surfaces were inspected in a MicroProf white light profilometer from the Fries Research & Technology (Bergisch Gladbach, Germany) and in SEM (JSM-6300 of Jeol, Tokyo, Japan). Prior to SEM investigation at high acceleration voltages the specimens were sputtered with an Au/Pd alloy using a device of Balzers (Lichtenstein).

Results and discussion

Universal hardness

For both EPDM and SBR rubbers, the universal hardness increases with increasing CB content (Table 1).

Friction and specific wear rate

The COF (line) and the specific wear rate (column) of the EPDM and SBR rubbers with varying CB contents measured in Orbital-RBOP and Oscillating-RBOP configurations, respectively, are summarized in Fig. 2. One could get the impression that incorporation of CB increases the COF marginally and decreases the specific wear rate. Note that the COF in Orbital-RBOP configuration is higher than that in Oscillating-RBOP for both EPDM and SBR systems.

In Orbital-RBOP, already 30 phr CB reduces the specific wear rate markedly compared to the neat materials. This note holds for both EPDM and SBR. In Oscillating-RBOP, the specific wear rate seems to decrease monotonously with increasing CB content for both EPDM and SBR rubbers.

Table 1 Universal hardness of EPDM and SBR materials

	EPDM				SBR			
	0	30	45	60	0	30	45	60
Universal hardness H (MPa)	1.8	3.4	7.2	8.2	1.2	2.7	4.7	8.8

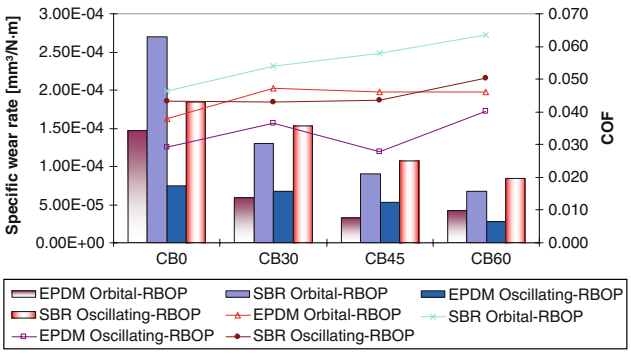

Fig. 2 Changes of the COF (line) and the specific wear rate (column) for EPDM and SBR in Orbital-RBOP and Oscillating-RBOP configurations as a function of CB content

Wear mechanisms

EPDM: Orbital-RBOP

SEM pictures taken from the worn surface of EPDM0 after Orbital-RBOP test are shown in Fig. 3. Since the ball in the rig is guided by a bearing ring, fixed at a motor shaft, it rotates with concentric revolutions and spins at the same time. As a consequence, the wear track can be different and divided into three regions. Each region has its own characteristics, Fig. 1 [12]. Figure 3 shows the regions with additional forward spin (outer region, Fig. 3a), backward spin of the ball (inner region, Fig. 3c), and the midsection between the above two regions (center region, Fig. 3b), respectively. In the outer region, massive cracking occurs which is likely due to the missing CB reinforcement. In the center, debris are accumulated. In the inner region, ploughing, tearing events dominate.

Incorporation of 30 phr CB changes the wear mechanisms fundamentally—a Schallamach pattern appears in the outer region. This is in accord with a reduced specific wear rate compared to that of EPDM0. Schallamach waves develop when the contact region in the rubber is subjected to tangential forces. The waves cross the contact region at a speed higher than that of the sliding/rolling counterpart. This can only happen when the contact between the rubber and steel ball is repeatedly and temporarily lost [13]. The wave fronts are more or less transversely oriented to the rolling direction (Fig. 4a). Further incorporation of CB in EPDM reduces the space between two neighboring waves and favors roll formation. Besides, some pitting events can be discerned in the wavy pattern (Fig. 4d). The accumulation of fragments is still the characteristic for the center region where the spin of the ball is negligible (Fig. 4b).

Fibrils are found in the inner region of the rolling wear track of EPDM30 (Fig. 4c). They might have been formed by tearing and rolling from earlier developed Schallamach waves. The onset of fibrils always suggests some thermal/

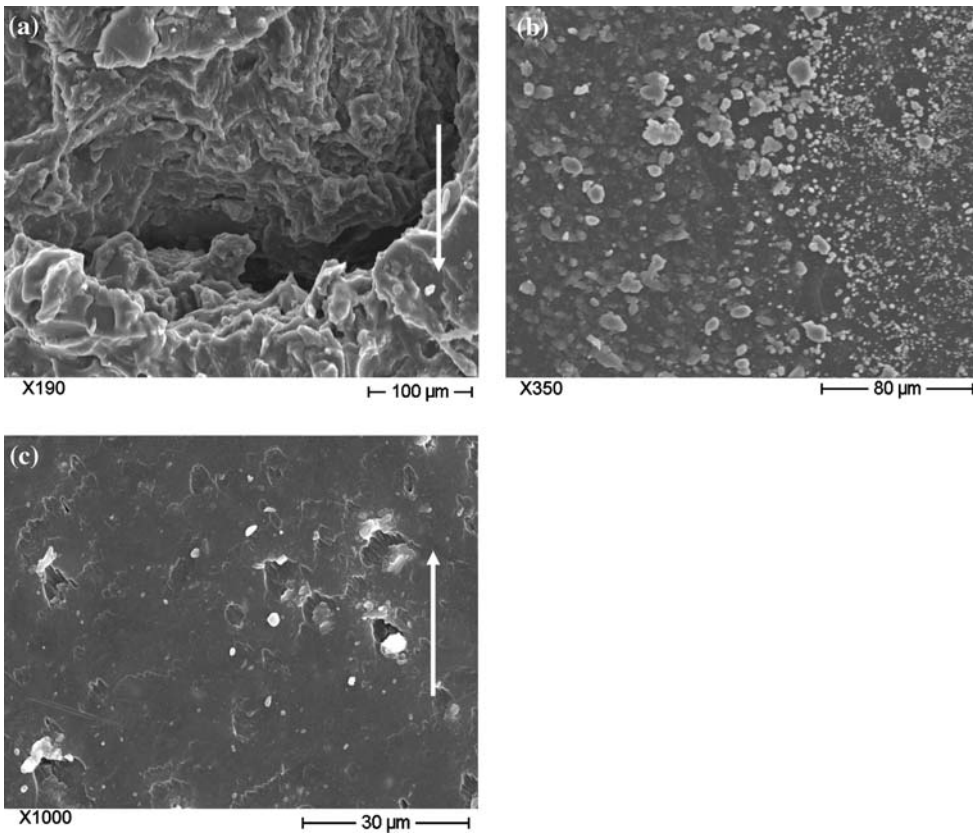

Fig. 3 SEM pictures taken from the rolling wear track of EPDM0 after Orbital-RBOP test. (**a**) Outer region, (**b**) center region, and (**c**) inner region. *Note*: The direction of the relative sliding speed of the ball against the rubber is shown by the arrows

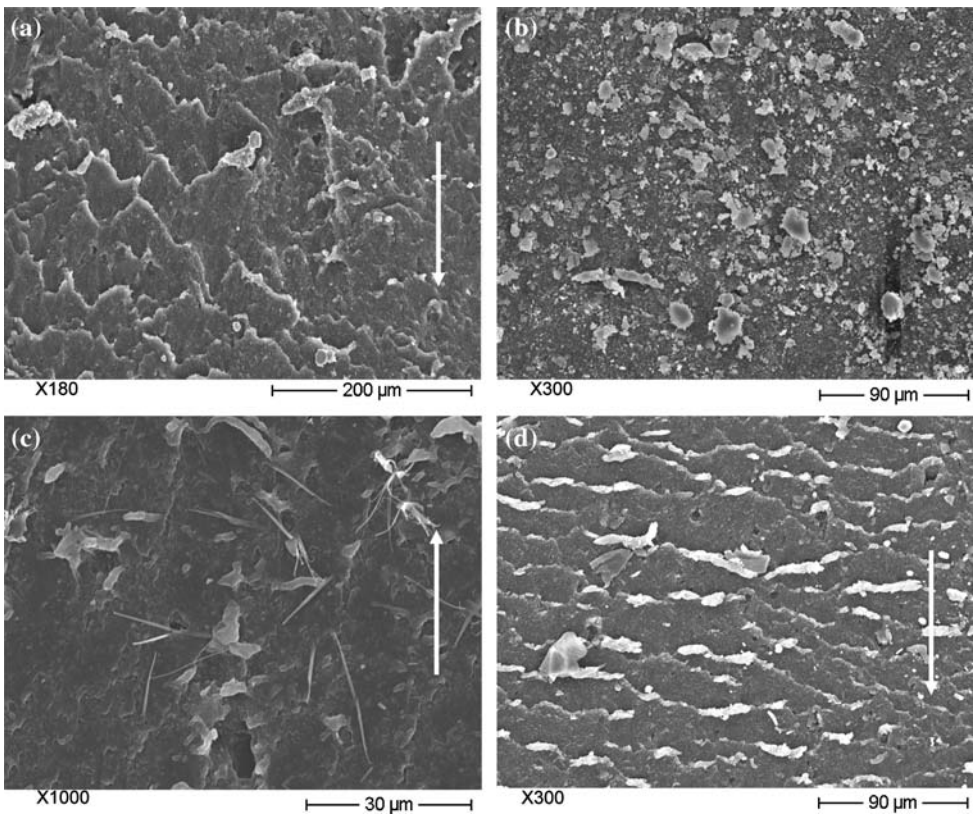

Fig. 4 SEM pictures taken from the rolling wear tracks of EPDM30 (**a**–**c**) and EPDM60 (**d**) after Orbital-RBOP tests. (**a**) Outer region, (**b**) center region, (**c**) inner region, and (**d**) outer region. *Note*: The direction of the relative sliding speed of the ball against the rubber is shown by the arrows

tribochemical effects due to which the rubber is decomposed and thus well adhered to the ball. When the ball rotates away, the rubber surface tears and yields some fibrillar structure which is disrupted further on [12].

EPDM: Oscillating-RBOP

With the Hertzian theory, the pressure distribution over the contact area can be estimated [14]. Accordingly, the wear track is divided into three regions: two side and one center regions (Fig. 5). Figure 6 shows an abrasion-type pattern (which have been demonstrated in detail in [15–17]) and formation of large cracks occurring in the side regions of the rolling wear track of EPDM0. No such type of feature was observed in other Oscillating-RBOP tests. Pitting, debris agglomeration and their "ironing" are discerned in the center region (Fig. 6c, d). The pitting is likely due to fatigue-induced cracking caused by the repeated cyclic pressure exerted on the surface layer of the rubber by the steel ball.

Fatigue-induced damage associated with pitting, flattened particles and fibrils can be observed in the wear track of EPDM60 after Oscillating-RBOP test (Fig. 7). The onset of fibrils has probably the same reason as mentioned before with respect to Orbital-RBOP. The overall smooth surface of EPDM60 accounts for its smaller specific wear rate compared to EPDM0.

SBR: Orbital-RBOP

SEM pictures taken from the worn surface of SBR0 after Orbital-RBOP test are shown in Fig. 8. In the outer region, less developed Schallamach pattern appears (Fig. 8a). At higher magnification, it is seen that the wear is rather complex with hints for cutting and detachment of small fragments (fragmentation) (Fig. 8b). In the center and inner regions very large agglomerates are formed (Fig. 8c, d). On the worn surface of the wear track, smooth surface is found, which might have been generated by the spalling of the rubber under shear stress (Fig. 8e). After the friction experiment the whole surface of the wear track has a dark, oily appearance (Fig. 8f). This should be linked with surface degradation, decomposition of the rubber. This is likely caused by the locally very high flash temperatures. This is the right place to mention that the heat development was detected by an infrared thermocamera. The temperature rise in Orbital-RBOP and Oscillating-RBOP configurations was <13 and <3 °C, respectively. Note that this difference correlates with that of the rolling speed (cf. experimental section).

Incorporation of 30 phr CB reduces the width between the Schallamach waves. At the same time the height of the waves also becomes smaller (Fig. 9a). In the outer region, the wave fronts with roll head are clearly observed (Fig. 9a). Higher magnification picture indicates that wear happens in a complex way covering shearing, roll formation and fragmentation (Fig. 9b). Fragmentation and small scale pitting are the basic wear mechanisms for the center and inner region of the wear track of SBR30 (Fig. 9c, d).

No Schallamach pattern was found on the surface of SBR45 or SBR60. Increasing amount of CB inhibits the occurrence of the Schallamach pattern. This is probably the reason for the decreased specific wear rate found.

For SBR45 an uncracked surface layer was observed (Fig. 10). This is quite unexpected and suggests fatigue-type initial damage. A similar phenomenon has been found

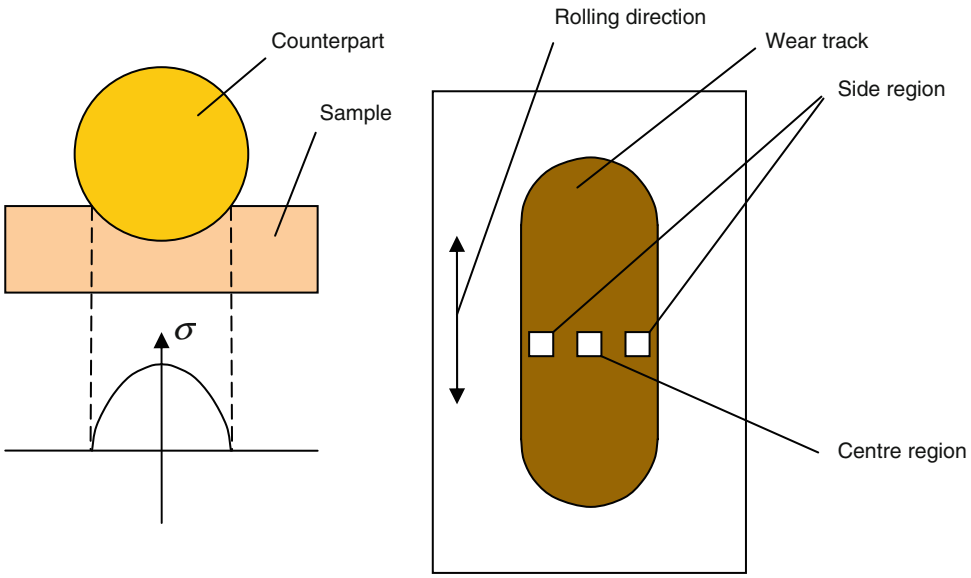

Fig. 5 Hertzian pressure distribution over the contact area and three regions designated for Oscillating-RBOP

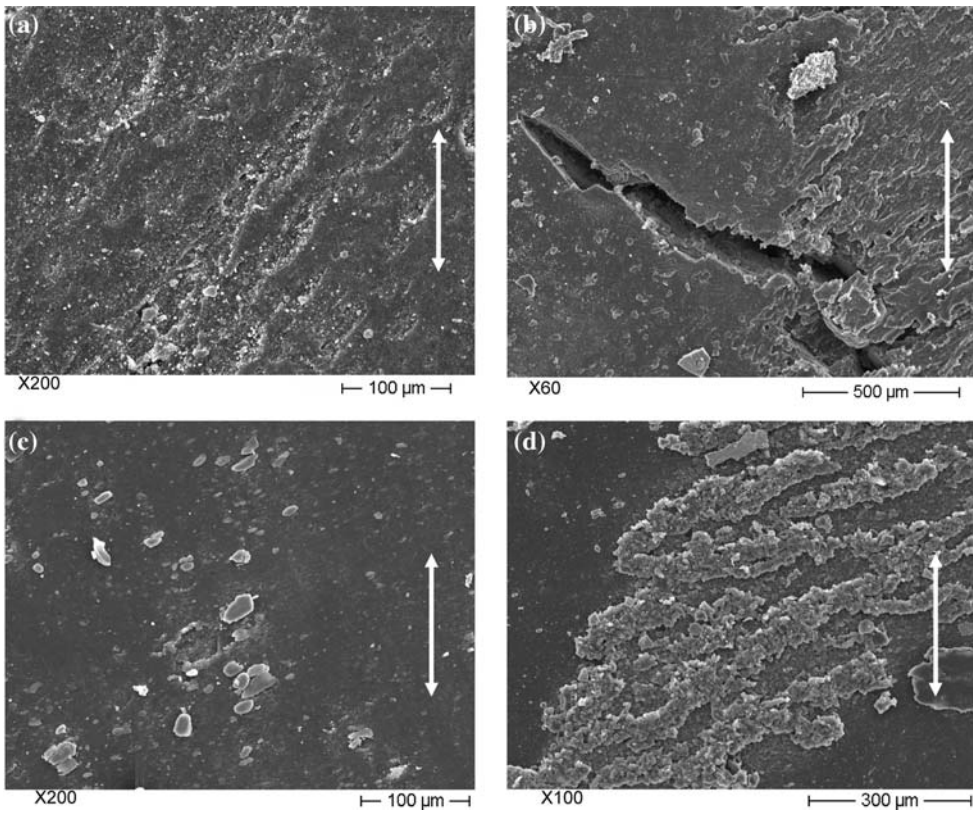

Fig. 6 SEM pictures taken from the rolling wear track of EPDM0 after Oscillating-RBOP test. (**a**) Abrasion pattern in side region, (**b**) cracking in side region, (**c**) pitting in center region, and (**d**) agglomerate formation and their "ironing" in the center region. *Note*: Rolling direction is shown by the arrows

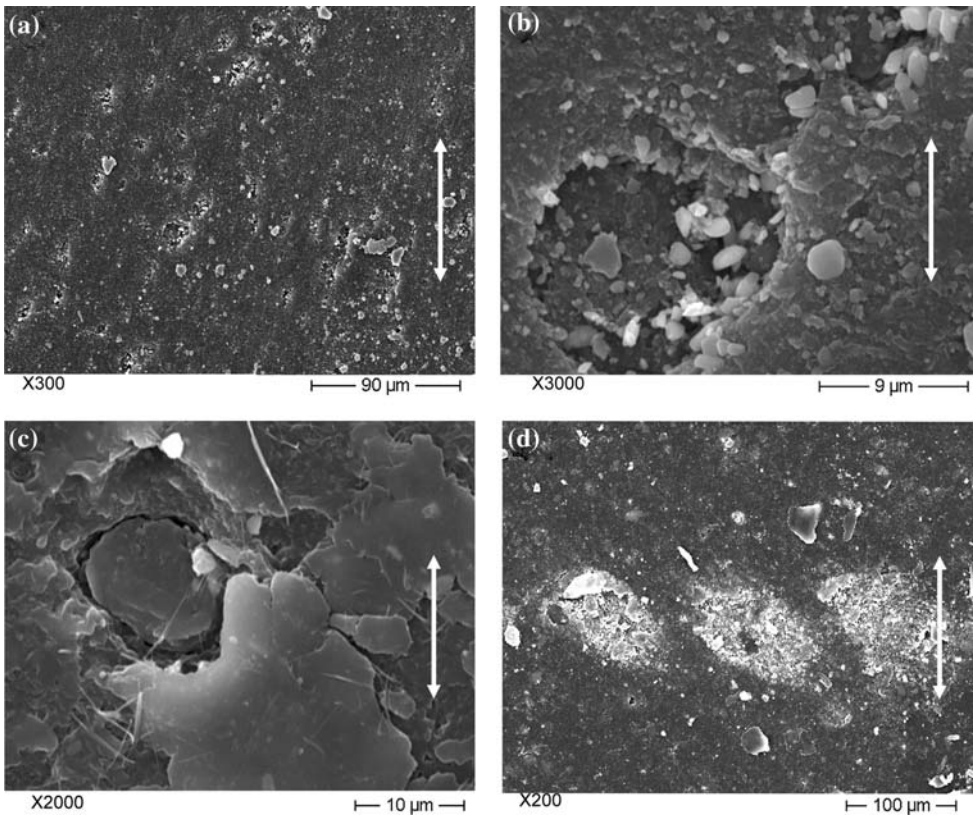

Fig. 7 SEM pictures taken from the rolling wear track of EPDM60 after Oscillating-RBOP test. (**a**) Side region, (**b**) pitting in side region, (**c**) fatigue-induced surface cracking and fibril formation in side region, and (**d**) center region. *Note*: Rolling direction is shown by the arrows

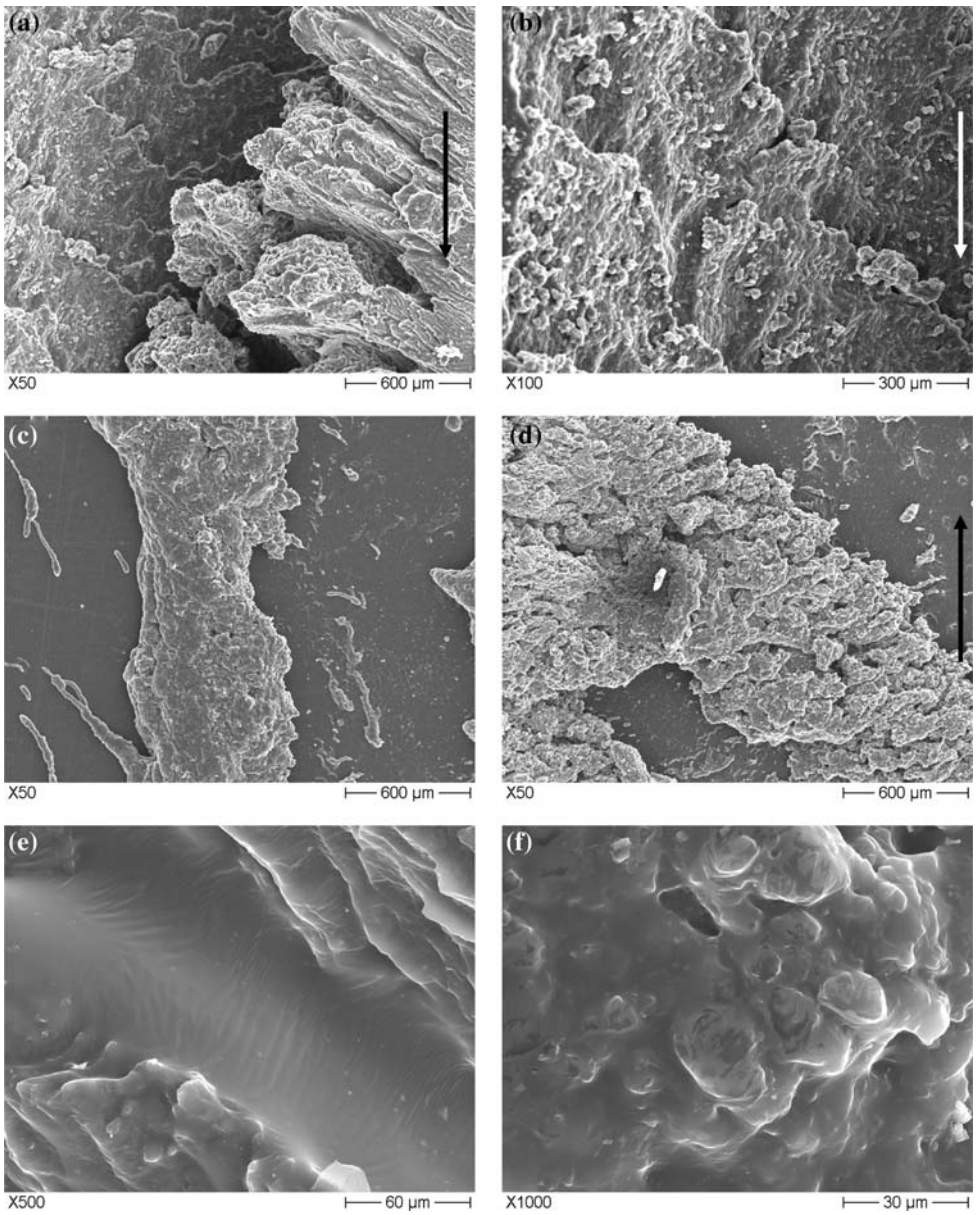

Fig. 8 SEM pictures taken from the rolling wear track of SBR0 after Orbital-RBOP test. (**a**, **b**) Outer region, (**c**) center region, (**d**) inner region, (**e**) shear surface in the wear track, and (**f**) oily surface. *Note*: The direction of the relative sliding speed of the ball against the rubber is shown by the arrows

for polyamide 66 [18]. Since no lubricant was used during the experiment, this surface layer seems to be composed of "softened" SBR45. Nevertheless its forming mechanism needs further investigation.

SBR: Oscillating-RBOP

Figure 11 shows the worn surfaces of SBR0 and SBR60 after Oscillating-RBOP tests. For SBR0, fragments and agglomerates are the main characteristics in the side and center regions, respectively (Fig. 11a, b). For SBR60, few ironed particles and pitting holes can be traced (Fig. 11c, d). Note that the overall wear track is quite featureless. This change in the wear mechanisms is in line with the reduction of the specific wear rate of SBR60 compared to the compounds containing less CB.

By analyzing all SEM photos taken from the EPDM and SBR systems, we can notice that fibrils appear only in CB containing EPDM mixes. Because the fibrils were found in both Orbital- and Oscillating-RBOP, their occurrence is not sensitive to the experimental conditions, but depends on the properties of the rubbery material. This claim is confirmed by the fact that fibril formation was observed for CB containing EPDM also due to dry sliding [19].

It can also be established that the reason why the COF measured in Oscillating-RBOP is lower than that measured in Orbital-RBOP lies in the movement of the ball. The ball in Orbital-RBOP rotates with an additional spin. It removes

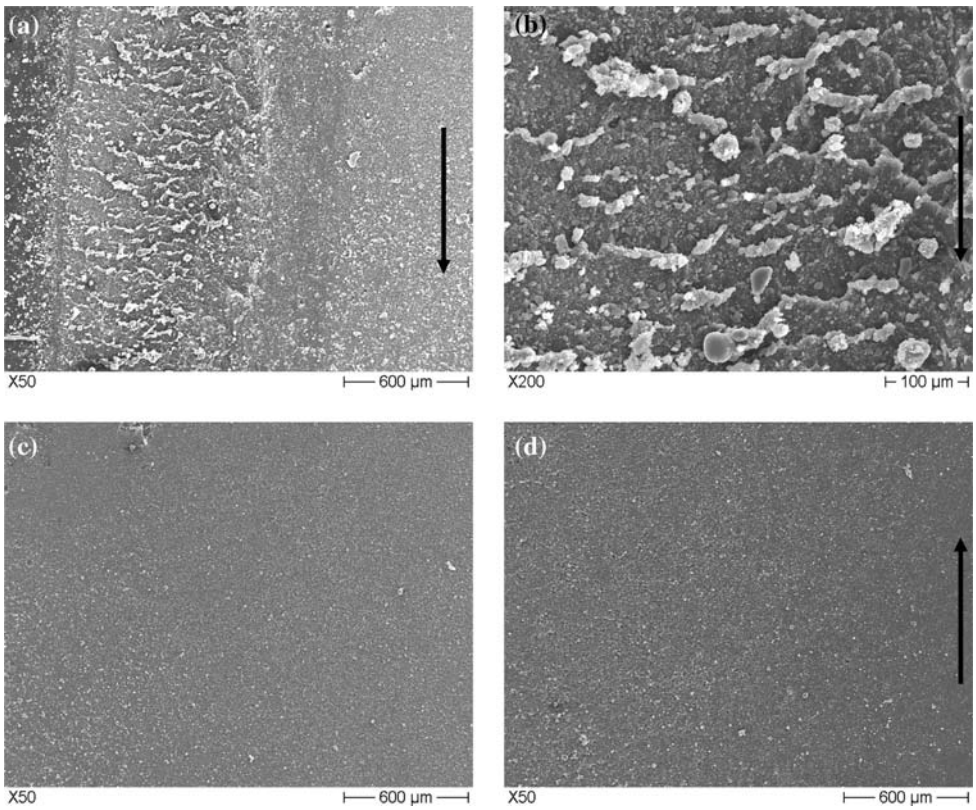

Fig. 9 SEM pictures taken from the rolling wear track of SBR30 after Orbital-RBOP test. (**a**, **b**) Outer region, (**c**) center region, and (**d**) inner region. *Note*: The direction of the relative sliding speed of the ball against the rubber is shown by the arrows

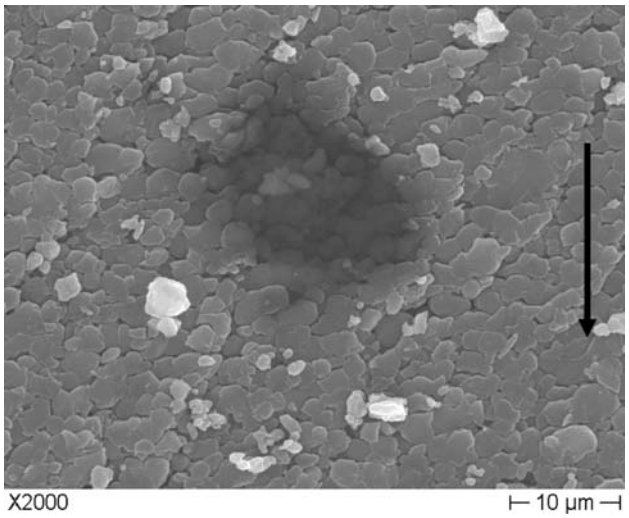

Fig. 10 A uniform filling taken from the rolling wear track of SBR45 after Orbital-RBOP test. *Note*: The direction of the relative sliding speed of the ball against the rubber is shown by the arrow

the debris from the ball's way and exerts additional resisting force to the ball.

Correlation between specific wear rate and universal hardness

Between specific wear rate and universal hardness a power law function could be deduced (see Eq. 2) (Fig. 12).

$$W_s = kH^{-n} \tag{2}$$

where W_s [mm^3/N m] is the specific wear rate, H [MPa] is the universal hardness, k and n are constants. k and n (collected in Table 2) differ for different rubbers and testing rigs.

One may notice that there is a strong similarity between Eq. 2 and the Archard's equation [20], the generalized form of the latter (Eq. 3) proved to be valid for the sliding wear of very different materials [21].

$$W_s \propto \frac{p^{\alpha} v^{\beta}}{H^{\lambda}} \tag{3}$$

where p is the contact pressure, v is the relative sliding velocity, H is the material hardness, and α, β, and γ are constants. Recall that in case of the Archards's law $\alpha = \beta = \gamma = 1$.

Note that for the same rubber k and n are different for Orbital-RBOP and Oscillating-RBOP conditions (Table 2). The most likely explanation for this, well reflected by the correlation lines in Fig. 12, is linked with the difference in the corresponding rolling speeds. This speed difference causes the prominent difference in the temperature rise observed. However, apart from the speed, the motion of the rolling ball should also be considered to interpret the changes in the wear mechanisms between Orbital-RBOP and Oscillating-RBOP. Anyway, the correlation given by Eq. 2 is holding for many rubbers tested by us so far under ball rolling wear conditions.

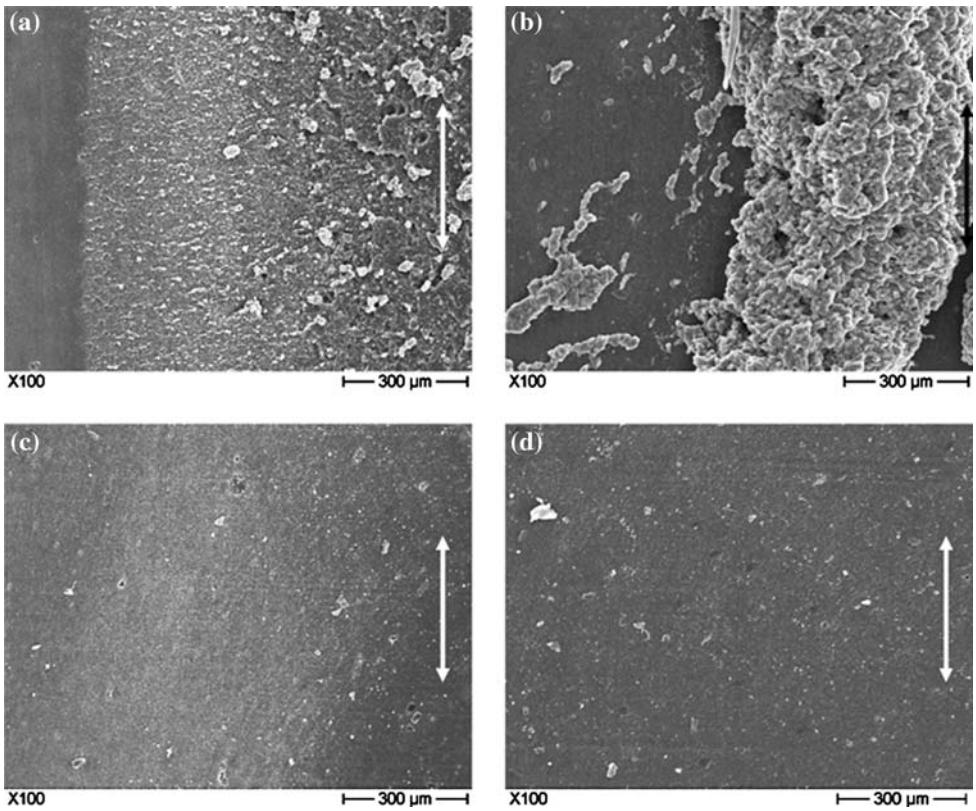

Fig. 11 SEM pictures taken from the rolling wear tracks of SBR0 (**a**, **b**) and SBR60 (**c**, **d**) after Oscillating-RBOP tests. (**a**, **c**) Side region and (**b**, **d**) center region. *Note*: Rolling direction is shown by the arrows

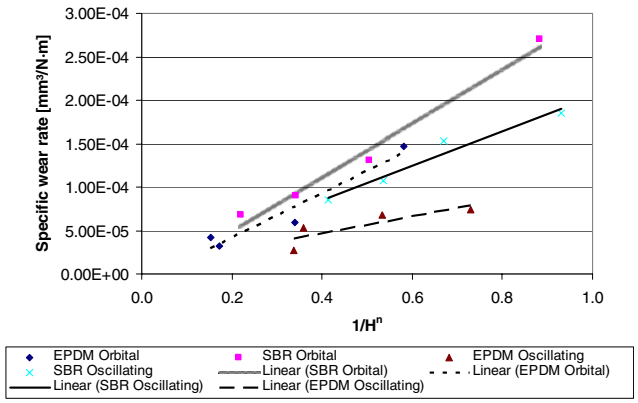

Fig. 12 Relationship between specific wear rate (W_s) and universal hardness (H)

Table 2 k and n for EPDM and SBR

	k	n
Orbital-RBOP		
EPDM	0.0002	0.8931
SBR	0.0003	0.6961
Oscillating-RBOP		
EPDM	0.0001	0.5185
SBR	0.0002	0.4052

Conclusions

Based on the work devoted to determine the dry rolling friction and wear behaviors of EPDM and SBR rubbers with various CB contents against steel counterpart in different test rigs (Orbital-RBOP and Oscillating-RBOP), the following conclusions can be drawn:

- Universal hardness of either EPDM or SBR increases with increasing CB content.
- Incorporation of CB increases marginally the COF and decreases the specific wear rate. The COF in Orbital-RBOP configuration is larger than that in Oscillating-RBOP for both EPDM and SBR.
- An inverse power law function was proposed between specific wear rate of rolling wear and universal hardness. So, a better resistance to rolling wear can be predicted for a rubber with higher universal hardness.

Acknowledgements D. Xu thanks the DFG (German Science Foundation) for her fellowship (Graduate school GK 814). Part of this work was done in the framework of the EU project "Kristal" (Contract no.: NMP3-CT-2005-515837; www.kristal-project.org).

References

1. Slusarski L, Bielinski DM, Affrossman S, Pethrick RA (1998) Kautschuk, Gummi, Kunststoffe 51:429
2. Wildberger A, Geisler H, Schuster RH (2007) Kautschuk, Gummi, Kunststoffe 60:24
3. Hong CK, Kim H, Ryu C, Nah C, Huh YI, Kaang S (2007) J Mater Sci 42:8391. doi:10.1007/s10853-007-1795-3
4. Majumder PS, Bhowmick AK (1998) Wear 221:15. doi:10.1016/S0043-1648(98)00255-5
5. Zhang SW (2004) Tribology of elastomers. Tribology and interface engineering series, No. 47. Elsevier B. V., New York
6. Friedrich K (1986) Friction and wear of polymer composites, vol 1. Composite materials series. Elsevier science publishers B. V., Amsterdam, The Netherlands
7. Bayer RG (2002) Wear analysis for engineers. HNB Publishing, New York
8. Thavamani P, Khastgir D, Bhowmick AK (1993) J Mater Sci 28:6318. doi:10.1007/BF01352190
9. Thavamani P, Bhowmick AK (1993) J Mater Sci 28:1351. doi:10.1007/BF01191977
10. Iwai T, Hasegawa K, Ueda S, Uchiyama Y (2005) J Jpn Soc Tribol 50:620
11. Universal hardness test. German norm (1997)
12. Felhös D, Karger-Kocsis J, Xu D (2008) J Appl Polym Sci 108:2840. doi:10.1002/app.27624
13. Schallamach A (1971) Wear 17:301. doi:10.1016/0043-1648(71)90033-0
14. Sarkar AD (1980) Friction and wear. Academic Press Inc. Ltd., London
15. Fukahori Y, Yamazaki H (1994) Wear 171:195. doi:10.1016/0043-1648(94)90362-X
16. Fukahori Y, Yamazaki H (1994) Wear 178:109. doi:10.1016/0043-1648(94)90135-X
17. Schallamach A (1958) Wear 1:384. doi:10.1016/0043-1648(58)90113-3
18. Chen YK, Kukureka SN, Hooke CJ, Rao M (2000) J Mater Sci 35:1275. doi:10.1023/A:1004709125092
19. Karger-Kocsis J, Mousa A, Major Z, Békési N (2008) Wear 264:359. doi:10.1016/j.wear.2007.03.021
20. Archard JF (1953) J Appl Phys 24:985. doi:10.1063/1.1721448
21. Zhu D, Martini A, Wang W, Hu Y, Lisowsky B, Wang QJ (2007) Trans ASME 129:544. doi:10.1115/1.2736439